Resonant transport in pulsated devices: Mobility oscillations and diffusion peaks

Marcello Borromeo[1,2] and Fabio Marchesoni[2,3]
[1]*Dipartimento di Fisica, Università di Perugia, I-06123 Perugia, Italy*
[2]*Istituto Nazionale di Fisica Nucleare, Sezione di Perugia, I-06123 Perugia, Italy*
[3]*Dipartimento di Fisica, Università di Camerino, I-62032 Camerino, Italy*
(Received 5 September 2008; published 24 November 2008)

Diffusion of an overdamped Brownian particle on a symmetric periodic substrate is investigated in the presence of pulsated perturbations of two kinds: (i) Stepwise lateral displacements (flashing substrate) and (ii) instantaneous tilts (shot noise). Pulses are applied, as it is often observed, in either periodic or random sequences with assigned mean (bias) and average waiting time (time constant). For a given bias, both the diffusion coefficient and the mobility of the particle can be greatly enhanced by tuning the time constant. Moreover, also depending on the time constant, the mobility can grow negative in (i) or exceed unity in (ii). We term this phenomenon resonant transport.

DOI: 10.1103/PhysRevE.78.051125 PACS number(s): 05.60.−k, 66.10.C−, 82.75.−z

I. INTRODUCTION

Brownian diffusion in a periodic substrate is often associated with a jittering dynamics which results from (Fig. 1) (i) model A, instantaneous lateral shifts of the substrate (flashing substrate); and (ii) model B, external kicks corresponding to instantaneous substrate tilts (shot noise). Both mechanisms have been largely employed to model transport at the micro-cale and nanoscale [1–3]. Prominent applications of model A include molecular motors at the cellular level [4,5], where flashing is caused by power strokes from the chemical energy source (like the hydrolysis of a single adenosine triphosphate molecule), tunable optical lattices for cold atoms [6–9], where substrate shifts are associated to degenerate atomic levels, and electromechanical sieves, e.g., for the electrophoresis of DNA strands [10–12]. Models of type B have also been around for a while: Introduced first to interpret the output of classical electronic devices [13], recently they have been employed to engineer quantum devices subject to shot noise of either electronic [14] or photonic nature [15].

A. Model A: Flashing substrate

To best summarize our conclusions, we first formulate the realizations of models A and B that we actually simulated. Let x be the coordinate of an overdamped Brownian particle of unit mass diffusing on the cosine potential

$$V(x) = d\,[1 - \cos(2\pi x/L)]. \tag{1}$$

In the following we set, for convenience, $d=1$ and $L=2\pi$. In model A the substrate shifts sidewise over time [16], i.e.,

$$V(x) \to V[x - X(t)], \tag{2}$$

where the drift $X(t)$ is either a square wave,

$$X(t) = x_0 \sum_{t_i \leqslant t} (-1)^i \Theta(t - t_i) \tag{3}$$

(zero-bias drift), or a staircase,

$$X(t) = x_0 \sum_{t_i \leqslant t} \Theta(t - t_i) \tag{4}$$

(unidirectional drift). Here $\Theta(x)$ is a Heaviside step function, $\{t_i\}$ is the sequence of the switch times, and $x_0 > 0$ is the step amplitude or length. We simulated both constant waiting times, $t_{i+1} - t_i \equiv \tau$ for any i (periodic sequence), and exponentially distributed waiting times, with time constant $\tau = \langle t_{i+1} - t_i \rangle$ (random sequence). In conclusion, model A is summarized by the Langevin equation (LE)

$$\dot{x} = -\sin[x - X(t)] + \xi(t), \tag{5}$$

where $\xi(t)$ is a Gaussian zero-mean noise with autocorrelation function $\langle \xi(t)\xi(0) \rangle = 2kT\delta(t)$, which maintains the system at the equilibrium temperature T.

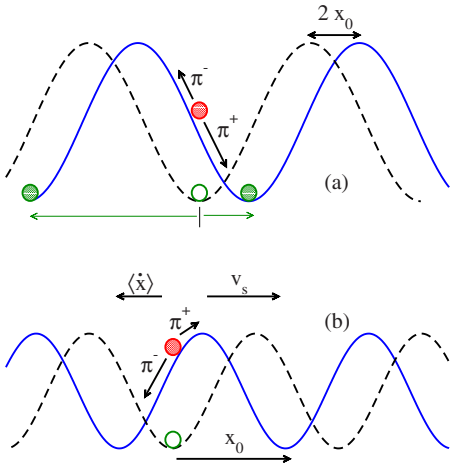

FIG. 1. (Color online) (a) Resonant diffusion. As the substrate switches between V_- (dashed curve) and V_+ (solid curve), in model A a particle initially at rest in a V_- well (empty green circle) gets instantaneously activated (red circle) and then diffuses either to the right or to the left (filled green circles) with probabilities $\pi_\pm$. (b) Negative mobility (model A). As the substrate advances to the right with average speed v_s, the activated particle (red circle) may happen to preferably roll backwards with $\pi_- > \pi_+$.

B. Model B: Kicked particle

Model B is defined by the spatial variable transformation $x \to y - X(t)$: Accordingly, the LE (5) becomes

$$\dot{y} = -\sin y + F_S(t) + \xi(t), \tag{6}$$

where $F_S(t) \equiv -\dot{X}(t)$ can be regarded as a shot noise acting upon the Brownian particle of coordinate y, diffusing in the static cosine potential $V(y)$. Correspondingly, the zero bias, (3), and unidirectional drift, (4), are mapped into a sequence of δ-like spikes with alternate, $F_S(t) = -2x_0 \Sigma_{t_i<t}(-1)^i \delta(t-t_i)$, or equal signs, $F_S(t) = -x_0 \Sigma_{t_i<t} \delta(t-t_i)$. Moreover, due to the linear nature of the transformation $x \to y$, models A and B have the same diffusion coefficient D. For numerical purposes we computed D for model A, i.e., $D \equiv \lim_{t\to\infty}[\langle x^2(t)\rangle - \langle x(t)\rangle^2]/2t$.

C. Main results

In the current literature [13], the unidirectional drifts of model A and the unidirectional shot noises of model B are often characterized in terms of their time averages, respectively, the net drift velocity of the substrate, $v_s = x_0/\tau$, and the net driving force, $f_s = -x_0/\tau$, felt by the particle. In fact, this approach typically holds good for macroscopic devices, where τ is negligible with respect to the device response times. On the contrary, we show below that the interplay of time-pulsated perturbations and spatial periodicity may strongly affect particle transport in a small device. By tuning τ at constant bias, v_s or f_s, we observed the following:

(a) *Model A.* Negative mobility dips with $\mu_A \equiv \langle \dot{x}\rangle / v_s < 0$, indicating particles that drift with average velocity opposite to the substrate drift.

(b) *Model B.* Excess mobility peaks with $\mu_B \equiv \langle \dot{y}\rangle / f_s > 1$, implying that, for an appropriate τ, shot noise can push particles faster than in the absence of substrate barriers (in which case $\mu_B = 1$ [17]).

(c) Correspondingly, excess diffusion peaks with $D > kT$, which appear to anticipate both the dips, (a), and the peaks, (b), of the mobility curves. [In our notation the diffusion coefficient of a free Brownian particle (i.e., for $V \equiv 0$) is kT.]

(d) Finally, in both models, for zero bias ($v_s = f_s = 0$) and an appropriate τ interval, we observed a remarkable resonant diffusion effect, also with $D > kT$.

Properties (a)–(c), presented in Sec. III and property (d), anticipated in Sec. II, can be regarded as manifestations of a resonant transport mechanism controlled by the time constant of the pulse sequence. The persistence of this effect in the presence of continuous drifts $X(t)$ is briefly discussed in Sec. IV.

II. RESONANT DIFFUSION AT ZERO BIAS

We start now analyzing the results of our simulations for the processes (3) and (4) at zero bias. In Fig. 2 we display D/kT versus τ at different temperatures. The pulse sequences are periodic in panel (a) and random in panel (b). The resonant nature of the curves $D(\tau)$ is apparent in both panels, although more prominent for periodic sequences.

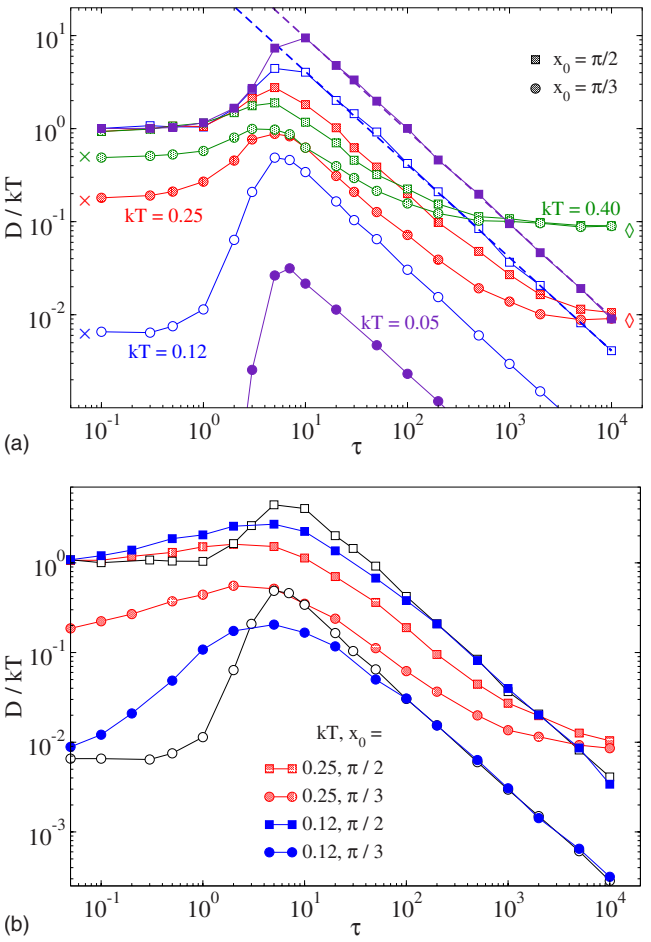

FIG. 2. (Color online) (a) Resonant diffusion D/kT vs τ for an unbiased pulsated substrate (same for models A and B). The square wave $X(t)$ is periodic in (a) and random in (b). The simulation parameters kT and x_0 are reported in the legend. Crosses and lozenges in (a) are the relevant analytical predictions for $\tau \to 0$ and $\tau \to \infty$, respectively (see text). The dashed lines in (a) represent the optimal diffusion law (7) for $x_0 = \pi/2$. Two data sets from (a) (blue symbols) have been reported in (b) (empty symbols) for the reader's convenience.

We interpret such an effect as a new instance of the so-called resonant activation phenomenon, originally demonstrated in bistable systems [18–20].

For exceedingly large τ, say, $\tau \to \infty$, Brownian diffusion achieves its asymptotic regime, $\langle x^2(t)\rangle - \langle x(t)\rangle^2 = 2D(\infty)t$, irrespective of the applied perturbation $X(t)$. The coefficient $D(\infty)$ thus coincides with the diffusion coefficient in the static, unbiased cosine potential $V(x)$, namely, $D(\infty) = kT\mu(d)$, where $\mu(d) = [I_0(d/kT)]^2$ is the relevant mobility, expressed in terms of the modified Bessel function $I_0(x)$ [17].

In the opposite limit, $\tau \to 0$, the diffusion process takes place in the effective potential $\bar{V}(x)$, obtained by time averaging either the sidewise switches $X(t)$ (model A) or the kicks $F_S(t)$ (model B). Upon implementing the vibrational mechanics scheme utilized in Refs. [21,22], one concludes that $\bar{V}(x)$ is still a cosine potential, but with rescaled amplitude $d \to d \cos x_0$. As a consequence, for vanishingly small τ, $D(0) = kT\mu(d \cos x_0)$. Our analytical estimates for $D(0)$ and

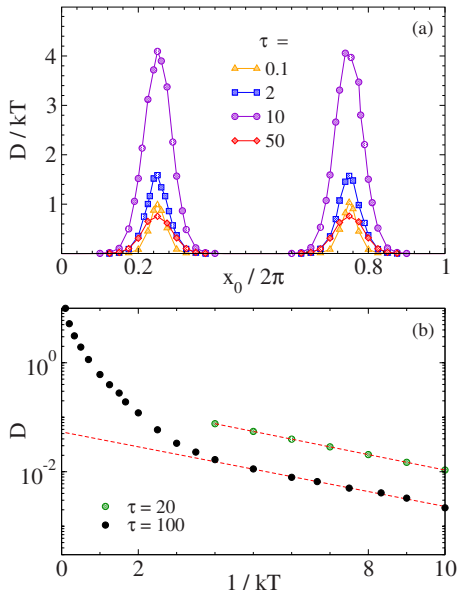

FIG. 3. (Color online) Diffusion coefficient D vs x_0 (a) and $1/kT$ (b) for different τ and vanishing bias (model A). Other simulation parameters: $kT=0.12$ in (a) and $x_0=\pi/3$ in (b). The $D(x_0)$ peaks in (a) are symmetric and periodic with period π. The dashed lined in (b) are our predictions (7) with $\pi_\pm$ given in Ref. [13] (see text).

$D(\infty)$ are also reported in Fig. 2(a). Note that, at variance with $D(\infty)$, $D(0)$ sharply depends on x_0. In particular, $D(0) \geqslant D(\infty)$ for any x_0 and $D(0)=kT$ (free diffusion) for $x_0=\pi/2$. Moreover, the unbiased LE (5) and (6) are invariant for $x_0 \to x_0+\pi$, as explicitly shown in Fig. 3(a).

The $D(\tau)$ curves bridge the two limits $D(0)$ and $D(\infty)$ by going through a broad resonance peak. Such excess diffusion peaks can be explained also by means of a simple argument. Let us consider, for instance, a substrate switch from $V_-(x) \equiv V(x+x_0)$ to $V_+(x) \equiv V(x-x_0)$ in model A. A particle initially sitting at a minimum of $V_-(x)$, now finds itself kicked a distance $2x_0$ to the left from the corresponding minimum of the shifted $V_+(x)$, as sketched in Fig. 1(a). In the overdamped regime, one can then introduce the splitting probabilities for the particle to relax toward the nearest $V_+(x)$ minimum to either the right, $\pi_+(x_0)$, or the left, $\pi_-(x_0)=1-\pi_+(x_0)$. The continuous particle dynamics (5) is thus mapped into a discrete random-walker process with [13]

$$D(\tau) = \frac{L^2}{2\tau}\pi_+(x_0)[1-\pi_+(x_0)]. \tag{7}$$

In the present case $L=2\pi$ and analytical expressions for $\pi_+(x_0)$ can be easily obtained as shown in Sec. 9.1 of Ref. [13].

This law fits well the decaying branch of our $D(\tau)$ curves. In Fig. 2(a) an explicit comparison is shown for the optimal choice $x_0=\pi/2$, corresponding to $\pi_\pm(x_0)=1/2$. In Fig. 3(b) we plotted D as a function of $1/kT$ for $x_0=\pi/3$ and two values of τ. The Arrhenius-like T dependence of the resonant diffusion branches is entirely due to the T dependence of $\pi_+(x_0)$ appearing in Eq. (7). In particular, the resonant D peaks get sharper and sharper as one lowers T.

Finally, as to be expected, a resonant D peak occurs at around the smallest time constant, τ_R, for which the optimal diffusion law (7) applies. Indeed, the random walker scheme leading to that law assumes implicitly that τ is no smaller than the relaxation time of a kicked particle towards the nearest potential minimum, so that, in our notation, $\tau_R \sim L/d = 2\pi$ [17].

The resonant diffusion effect illustrated in Figs. 2 and 3 should not be mistaken for the damped D oscillations induced by periodic bimodal [23] or trimodal additive symmetric forces [24] applied to a Brownian particle in a periodic potential. In Ref. [24] D/kT oscillations are reported for constant tilt amplitudes, F_0, as a function of the tilting time, t_t. In the notation of model B, (6), such finite-time tilting pulses are replaced here by instantaneous kicks of strength $x_0 = F_0 t_t$. As a consequence, the damped D oscillations reported in Ref. [24] must be regarded as the counterpart of the periodic oscillations of D versus x_0 displayed in Fig. 3(a) (damping being due to the finiteness of t_t). In this case, as well as in Ref. [23], we are in the presence of a commensuration effect between pulse strength x_0 and spatial periodicity of the substrate L, whereas resonant diffusion is rather controlled by the waiting time between consecutive kicks.

III. EXCESS MOBILITY AND DIFFUSION AT FINITE BIAS

We investigate now models A and B under the action of a unidirectional pulse sequence (4). In model A, the substrate drifts to the right with average speed $v_s=x_0/\tau$, while in model B, the shot noise has negative mean, $f_s=-v_s$. Owing to the transformation, $y=x-X(t)$, connecting the two processes (5) and (6), the relevant mobility functions, $\mu_{A,B}$, obey the identity $\mu_A=1-\mu_B$ (whereas, as mentioned above, D is the same). This means that excess peaks of μ_B correspond to negative dips of μ_A. Of course, in the absence of a substrate $\mu_B=1$ and $\mu_A=0$ for any choice of $X(t)$ [17].

In Fig. 4 we illustrate the bias dependence of D for different step lengths x_0. To demonstrate the symmetry of process (5) under the transformation $x_0 \to -x_0$ (mirror reflection) and $x_0 \to x_0+L$, with $L=2\pi$ (step-substrate commensuration), we displayed our diffusion data versus the reduced bias $[x_0]/\tau$, with $[x_0]=x_0 \bmod(2\pi)$. As a result, the data sets for $x_0=\pi/3$ and $7\pi/3$, and $x_0=2\pi/3$ and $4\pi/3$ collapse on two distinct curves.

The overall properties of such numerical curves can be summarized as follows. They all peak for $[x_0]/\tau$ in the vicinity of the substrate depinning threshold d (namely, the least force required to drag a noiseless particle over a substrate barrier). Diffusion enhancement is a general property of Brownian motion in a biased potential [25–27]. Being a threshold effect, diffusion enhancement peaks are associated to steps in the mobility curves (also shown in Fig. 4). (In the notation of model B the connection with the earlier literature is more apparent.) However, decreasing $[x_0]/\tau$ at constant x_0 means increasing τ, so that, at variance with the setup of Refs. [25–27], the pulsated nature of the drive now starts playing a role. Indeed, the linear tails, $D \propto [x_0]/\tau$, of Fig. 4 correspond to the linearly decaying branches (7) displayed in

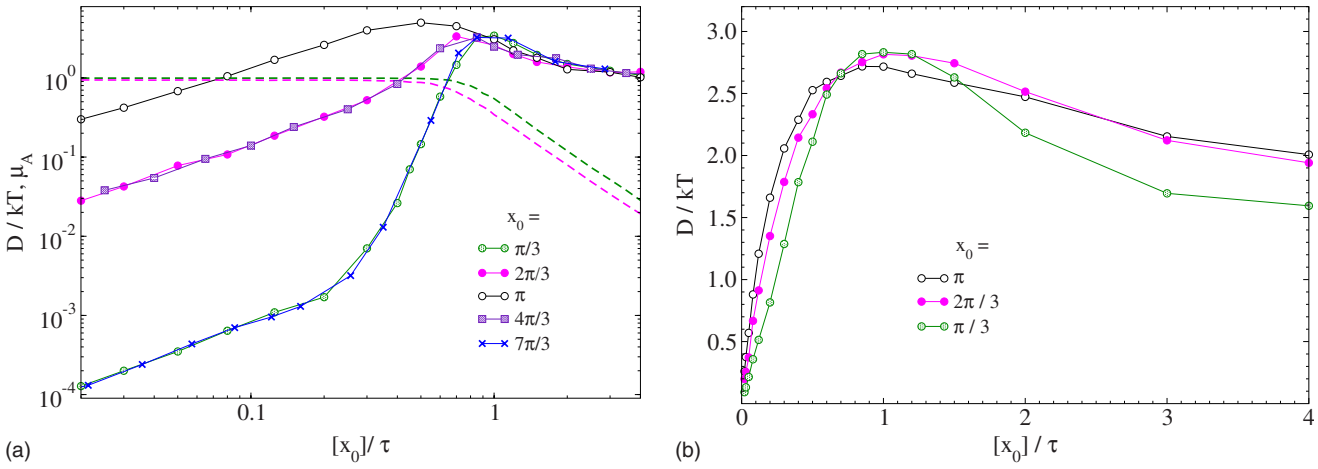

FIG. 4. (Color online) Transport on a sinusoidal substrate traveling with velocity $v_s=[x_0]/\tau$, where $[x_0]=x_0 \bmod(2\pi)$ (model A). The unidirectional step sequence is periodic in panel (a) and random in panel (b). x_0 was chosen to demonstrate the symmetry and under transformations $x_0\rightarrow -x_0$ and $x_0\rightarrow x_0+2\pi$ (see text). The relative diffusion coefficient is represented by circles and the mobility $\mu_A=\langle\dot{x}\rangle/v_s$ by dashed curves. For $x_0=\pi$ the mobility is zero within our numerical accuracy.

Fig. 2(a). For $[x_0]/\tau\rightarrow 0$ (not shown) all numerical curves eventually approach the asymptotic limit $D(\infty)$ for the zero-bias case. Finally, we stress that all of the above applies both to periodic (main panel) and random pulse sequences (inset), alike.

To illustrate the role of the drift time constant, in Fig. 5 we display our data for μ_A [panel (a)] and D [panel (b)] versus τ at constant bias v_s. The curves $\mu_A(\tau)$ exhibit damped oscillations with negative minima. This result may sound surprising if one considers that the substrate moves in the positive direction with $v_s>0$. However, when the substrate advances by one step length $x_0\gtrsim\pi$ to the right, a particle initially at rest is likely to get kicked into the well immediately to the left from its initial position and, thus, may drift with negative net velocity [Fig. 1(b)]. This mechanism applies for x_0 close to $(2m+1)\pi$, $m=0,1,2\ldots$, so that negative μ_A dips are expected for $\tau\simeq(2m+1)\pi/v_s$, in close agreement with our numerics. Extending this argument to model B also explains the observed excess μ_B peaks (not shown).

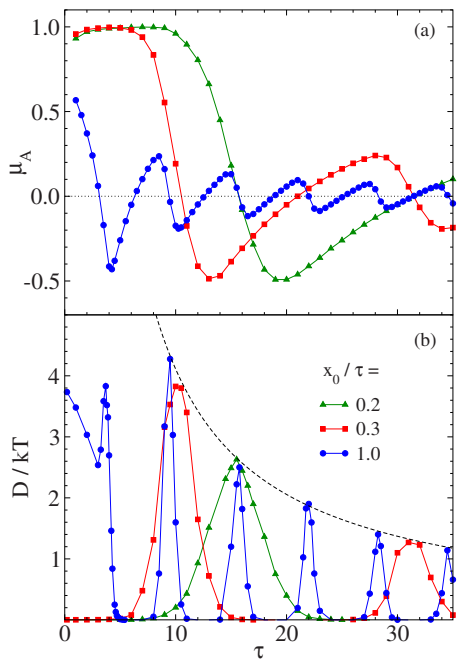

FIG. 5. (Color online) Transport enhancement induced by a period pulse sequence with fixed bias $v_s=x_0/\tau$ (model A) and varying τ. The mobility drops in (a) correspond to sharp diffusion peaks in (b). The dashed curve in (b) locates the maxima $\pi^2/2\tau$ of the resonant D.

In Fig. 5(b) we displayed the corresponding curves $D(\tau)$ for the same τ range as in Fig. 5(a): The coincidence between D peaks and μ_A drops is apparent, in agreement with the analysis of Ref. [25]. Most remarkably, the peaks for relatively large τ fall on the envelope curve $L^2/8\tau$, with $L=2\pi$, as one guesses by inspecting the linear D tails in Fig. 4. Such tails shift upwards on increasing x_0 from $2m\pi$ to $(2m+1)\pi$, so that the diffusion maxima in Fig. 5(b) must occur for $x_0=(2m+1)\pi$. The envelope curve drawn there is simply the optimal diffusion law (7) with $\pi_+[(2m+1)\pi]=1/2$.

IV. CONCLUDING REMARKS

We remark here that certain resonant transport features can be detected also in the presence of a continuous pulsated drift, for instance, the zero-bias sinusoidal function

$$X(t)=x_0\cos(\Omega t+\phi). \tag{8}$$

A variation of model B subject to a sinusoidal drift with tunable bias has been investigated in Ref. [28]. As mentioned at the bottom of Sec. III, the smoothness of the $X(t)$ wave form degrades the oscillations of the diffusion coefficient: At zero bias the D peaks in Fig. 3(a) are replaced by the kind of damped oscillations earlier reported in Ref. [24].

Most notably, in both models A and B, resonant curves of D versus $\tau\equiv 2\pi/\Omega$ emerge at zero bias and low temperatures (Fig. 6). The resonance peak is less pronounced with respect to that obtained by simulating a rectangular wave form (3). Moreover, the τ^{-1} branches of Fig. 4(a) are also

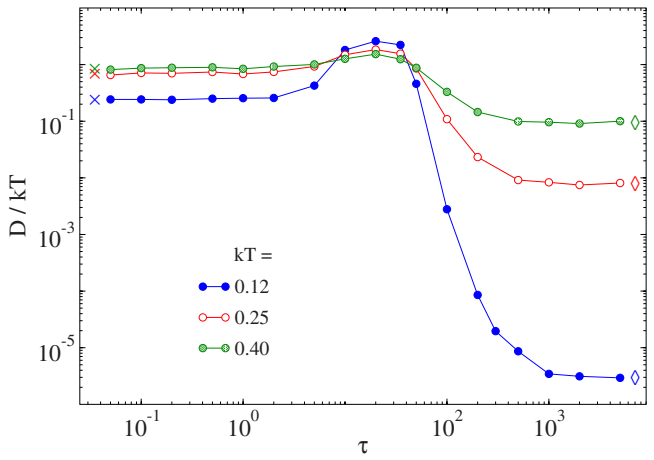

FIG. 6. (Color online) Resonant diffusion D/kT vs $\tau \equiv 2\pi/\Omega$ for a harmonically pulsated substrate at low temperatures. $X(t)$ given by Eq. (8) with $x_0=2\pi$ and $\phi=0$. Crosses and lozenges are the relevant analytical predictions for $\tau \to 0$ and $\tau \to \infty$, respectively, like in Fig. 2(a) (see text).

suppressed. Such curves are a signature of the diffusion enhancement induced by a periodic drive [29]. Similarly to Fig. 2(a), all $D(\tau)$ curves approach the free diffusion limit, $D(\infty)=kT\mu(d)$, and the vibrational mechanics limit, $D(0)=kT\mu[J_0(x_0/\Omega)d]$, respectively for extremely low and high modulation frequencies. [Here, $J_0(x)$ denotes a zeroth-order Bessel function [22].]

Finally, we remark that the combination of two (or more) harmonic components with commensurate frequencies, like

$$X(t) = x_1 \cos(\Omega_1 t + \phi_1) + x_2 \cos(\Omega_2 t + \phi_2), \tag{9}$$

with $\Omega_1/\Omega_2 = m/n$, $m,n=1,2,\ldots$, induces an additional rectification effect (not shown here), the magnitude and sign of which depend on the phase difference $\phi_2 - \phi_1$ (harmonic mixing [30]).

In summary, a particle diffusing on a pulsated periodic substrate, for appropriate combinations of the amplitude and frequency of the pulses, can synchronize its dynamics with the pulse sequence, which allows an effective control of the particle delivery (i.e., of both its speed and dispersion) [31]. When utilized in particle separation, such delivery control technique can be exploited to increase the separation speed and selectivity [2]. Preliminary estimates indicate that the simplest experimental setups to demonstrate the resonant diffusion mechanisms introduced here, are the optical potentials for colloidal particles investigated in Refs. [32,33]. Biology inspired devices, especially designed to control the transport of magnetic vortices in superconductors, can also provide an ideal playground for resonant diffusion experiments [34].

[1] P. Hänggi, F. Marchesoni, and F. Nori, Ann. Phys. **14**, 51 (2005).
[2] P. Hanggi and F. Marchesoni, http://www.citebase.org/abstract?id=oai:arXiv.org:0807.1283.
[3] P. Hänggi and F. Marchesoni, Chaos **15**, 026101 (2005).
[4] R. D. Astumian and P. Hänggi, Phys. Today **55**, 33 (2002).
[5] Y.-d. Chen, Phys. Rev. Lett. **79**, 3117 (1997).
[6] L. P. Faucheux, L. S. Bourdieu, P. D. Kaplan, and A. J. Libchaber, Phys. Rev. Lett. **74**, 1504 (1995).
[7] C. Mennerat-Robilliard, D. Lucas, S. Guibal, J. Tabosa, C. Jurczak, J.-Y. Courtois, and G. Grynberg, Phys. Rev. Lett. **82**, 851 (1999).
[8] R. Gommers, S. Bergamini, and F. Renzoni, Phys. Rev. Lett. **95**, 073003 (2005).
[9] R. Gommers, S. Denisov, and F. Renzoni, Phys. Rev. Lett. **96**, 240604 (2006).
[10] A. Ajdari and J. Prost, C. R. Acad. Sci., Ser. II: Mec., Phys., Chim., Sci. Terre Univers **315**, 1635 (1992).
[11] D. Ertas, Phys. Rev. Lett. **80**, 1548 (1998).
[12] T. A. J. Duke and R. H. Austin, Phys. Rev. Lett. **80**, 1552 (1998).
[13] C. W. Gardiner, *Handbook of Stochastic Methods* (Springer, Berlin, 1986).
[14] Y. M. Blanter and M. Büttiker, Phys. Rep. **336**, 1 (2000).
[15] C. H. Henry and R. E. Kazarinov, Rev. Mod. Phys. **68**, 801 (1996).
[16] M. Borromeo and F. Marchesoni, Phys. Lett. A **249**, 199 (1998).
[17] H. Risken, *The Fokker-Planck Equation* (Springer, Berlin, 1984).
[18] C. R. Doering and J. C. Gadoua, Phys. Rev. Lett. **69**, 2318 (1992).
[19] R. D. Astumian and M. Bier, Phys. Rev. Lett. **72**, 1766 (1994).
[20] M. Marchi, F. Marchesoni, L. Gammaitoni, E. Menichella-Saetta, and S. Santucci, Phys. Rev. E **54**, 3479 (1996).
[21] M. Borromeo and F. Marchesoni, Europhys. Lett. **72**, 362 (2005).
[22] M. Borromeo and F. Marchesoni, Phys. Rev. E **73**, 016142 (2006).
[23] H. Gang, A. Daffertshofer, and H. Haken, Phys. Rev. Lett. **76**, 4874 (1996).
[24] M. Schreier, P. Reimann, P. Hänggi, and E. Pollak, Europhys. Lett. **44**, 416 (1998).
[25] G. Costantini and F. Marchesoni, Europhys. Lett. **48**, 491 (1999).
[26] P. Reimann, C. Van den Broeck, H. Linke, P. Hänggi, J. M. Rubi, and A. Pérez-Madrid, Phys. Rev. Lett. **87**, 010602 (2001).
[27] B. Lindner, M. Kostur, and L. Schimansky-Geier, Fluct. Noise Lett. **1**, R25 (2001).
[28] M. Borromeo and F. Marchesoni, Phys. Rev. Lett. **99**, 150605 (2007).
[29] F. Marchesoni, Phys. Lett. A **231**, 61 (1997).
[30] F. Marchesoni, Phys. Lett. A **119**, 221 (1986).
[31] L. Machura, M. Kostur, P. Talkner, J. Łuczka, F. Marchesoni, and P. Hänggi, Phys. Rev. E **70**, 061105 (2004).
[32] Y. Roichman, V. Wong, and D. G. Grier, Phys. Rev. E **75**, 011407 (2007).
[33] W. Mu, Z. Li, L. Luan, G. C. Spalding, G. Wang, and J. B. Ketterson, J. Opt. Soc. Am. B **25**, 763 (2008).
[34] B. Y. Zhu, F. Marchesoni, and F. Nori, Physica E (Amsterdam) **18**, 318 (2003).